



Inelastic Neutron Scattering in Multiferroic Materials

N. M. Reynolds^{a,b}, P. Rovillain^{a,b}, P. Graham^a, A.M. Mulders^c, G. McIntyre^b, S. Danilkin^b,
K. Schmalzl^d, M. Reehuis^e, S. Miyasaka^f, J. Fujioka^f, Y. Tokura^f, B. Keimer^g, and C. Ulrich^{a,b}

^a*School of Physics, University of New South Wales, Sydney, Australia.*

^b*The Bragg Institute, ANSTO, Locked Bag 2001, Kirrawee DC NSW 2232, Australia.*

^c*School of Physical, UNSW, Canberra, ACT 2600 Australia.*

^d*Institut Laue Langevin, BP 156, 38042 Grenoble Cedex 9, France.*

^e*Helmholtz-Zentrum for Materials and Energy Berlin, Germany.*

^f*Department of Applied Physics, University of Tokyo, Tokyo 113-8656, Japan.*

^g*Max-Planck-Institute for Solid State Research Stuttgart, Germany.*

In order to obtain a deeper understanding of the spin interactions between the magnetic moments of the Tb-ions and the Mn-ions in multiferroic TbMnO₃, inelastic neutron scattering experiments (at the ILL in Grenoble and the Bragg Institute at ANSTO) are performed on isostructural, non-multiferroic TbVO₃. Acoustic and optical magnon branches are identified at energies comparable to the spin wave excitation spectrum of YVO₃. In addition, a crystal field excitation arising from the Tb-ions is identified at the energy of 14.9 meV. This is substantially larger than the crystal field excitation at 4.5 meV in TbMnO₃.

1. Introduction

Magnetism and ferroelectricity are both exciting physical properties and are used in everyday life in sensors and data storage [1]. Magnetic order occurs when the magnetic spin of the atoms are aligned in a periodic manner. Electric polarization is caused by a uniform displacement of an electronic configuration in a well defined direction. Multiferroic materials are materials where both properties coexist. They offer great potential for future technological applications such as increased data storage capacity or novel sensors. In principal, data storage capacity can be increased via the coexistence of electric and magnetic polarizations, thus replacing the current 2-bit system with a 4-bit memory system [2]. In some multiferroic materials, such as TbMnO₃, the two order parameters (electric polarization and magnetic order) are coupled. This allows for a direct switching of both properties. At present, the underlying mechanism for this coupling is not fully understood.

TbMnO₃ belongs to the class of orthorhombically distorted perovskites with the space group *Pbnm*. This structure consists of a network of corner-sharing MnO₆ octahedra with Tb-ions spaced between them. The octahedra are typically tilted and distorted, caused by the Jahn-Teller effect. The room temperature lattice parameters are $a = 5.30 \text{ \AA}$, $b = 5.86 \text{ \AA}$ and $c = 7.49 \text{ \AA}$ [3]. TbMnO₃ undergoes three magnetic phase transitions. Below 43 K the spins of the Mn-ions exhibit an incommensurate sinusoidal magnetic structure. Upon further cooling the spin structure changes at $T = 25 \text{ K}$ to a cycloidal spin structure where the spins rotate around the *a*-axis, i.e. within the *bc*-plane [4]. This phase transition is accompanied with the onset of the ferroelectric order. Finally, below 8 K the moments of the Tb-ions order ferromagnetically along the *b*-axis with an additional antiferromagnetic coupling between nearest-neighbor Tb-spins along the [110] direction [4]. In order to obtain a deeper understanding of the spin interactions between the Tb-moments and the Mn-moments, we have performed neutron



scattering experiments on the non-multiferroic material TbVO_3 . Both materials, TbMnO_3 and TbVO_3 , crystallize in the same three-dimensional perovskite crystal structure $Pbnm$, but possess a different electronic configuration, i.e. there are two electrons in the 3d electronic level of TbVO_3 in contrast to four in TbMnO_3 . The spin structure of TbVO_3 is C-type antiferromagnetic below 110 K [5-8], whereas the Tb-moments exhibit a non-collinear order below 11 K [8]. However, TbVO_3 does not exhibit an electric polarization down to the lowest temperatures.

2. Experimental details

Large high quality single crystals of TbVO_3 were grown by the travelling solvent floating-zone technique using an infrared mirror furnace. Details of the growth process are described by Miyasaka and Fujioka [5-7]. The inelastic neutron scattering experiments were performed on the triple-axis spectrometers IN8 and IN22 at the Institut Laue Langevin in Grenoble, France and at the instrument TAIPAN at the research reactor OPAL at ANSTO. A pyrolytic graphite PG 002 monochromator and analyzer were used with a setting of the final wavelength of $k_f = 2.662 \text{ \AA}^{-1}$. In order to suppress second order scattering, a PG-filter was placed before the analyzer.

3. Results

A contour plot of the inelastic neutron scattering data is presented in Fig. 1. The data were taken along the $(0,0,Q_L)$ direction starting from the zone centre $(\frac{1}{2}, \frac{1}{2}, 1)$ of the C-type antiferromagnetic Brillouin zone. Note that, as in ref. [9], the pseudo-cubic notation with $a^* = a/\sqrt{2}$, $b^* = b/\sqrt{2}$, and $c^* = c/2$ is used. The data were taken at 40 K, a temperature where the V-moments are ordered, but still above the magnetic ordering temperature of the Tb-sub-lattice. Three distinct branches are observed: a dispersive excitation between 5.0 meV and 12 meV, an intense and dispersionless excitation at 14.9 meV, and a weakly dispersive branch

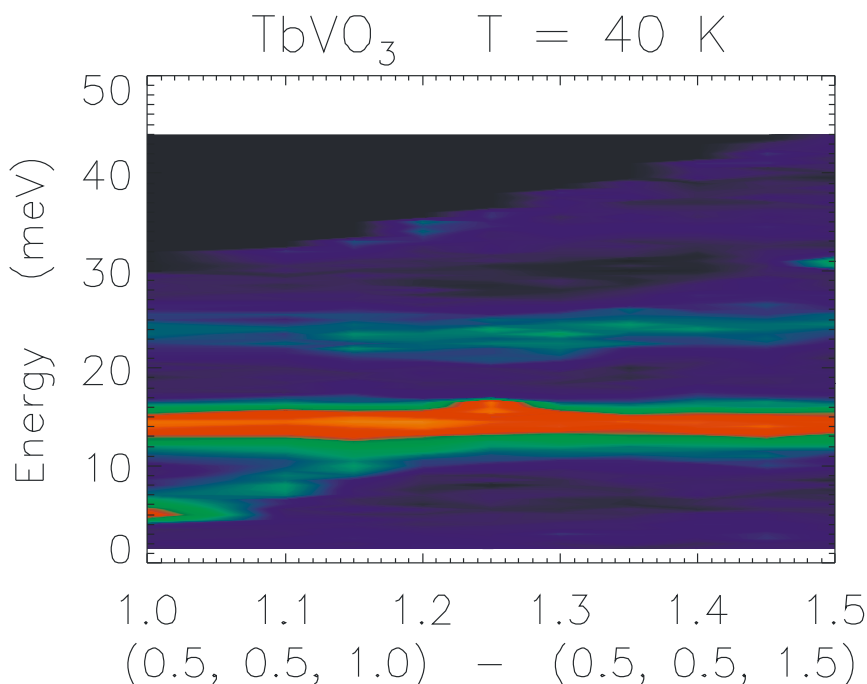


Fig. 1: Contour plot of the inelastic neutron scattering data of TbVO_3 along the $(0,0,Q_L)$ direction of the C-type antiferromagnetic Brillouin zone. The data were taken at a temperature of 40 K, i.e. within the C-type magnetic phase of TbVO_3 , but well above the ordering temperature of the Tb-moments.

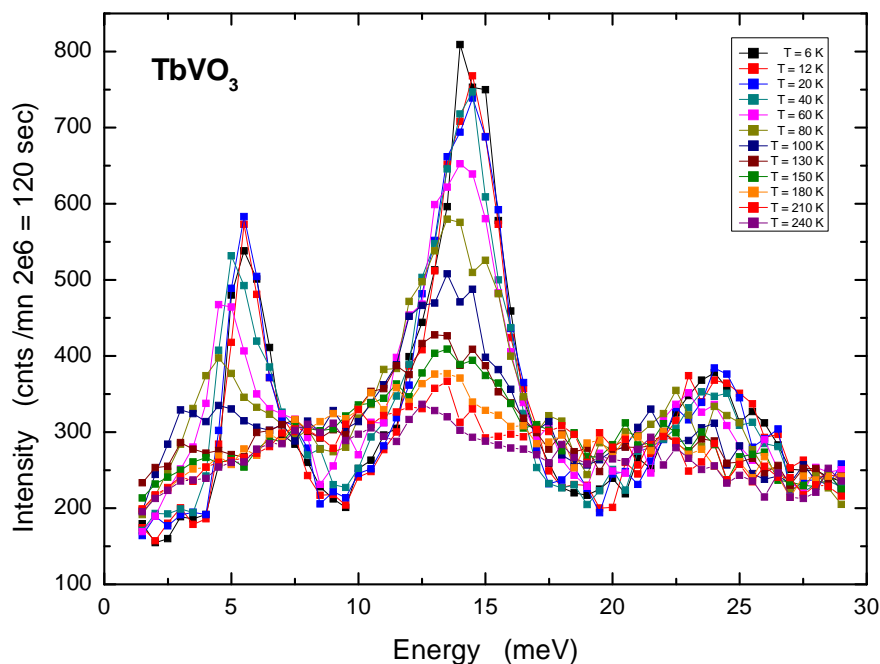


Fig. 2: Temperature dependence of the inelastic neutron scattering spectrum of TbVO_3 at the centre of the magnetic Brillouin zone, i.e. at $(\frac{1}{2}, \frac{1}{2}, 1)$.

between 24.3 meV and 25.6 meV. In order to identify the different excitations, we have investigated the temperature dependence of the inelastic neutron scattering spectrum at the centre of the magnetic Brillouin zone at $(\frac{1}{2}, \frac{1}{2}, 1)$.

Fig. 2 shows the temperature dependence of the spectrum at the centre of the C-type antiferromagnetic Brillouin zone. The peaks at 5.5 meV can be attributed to a spin wave excitation. This mode completely disappears at the magnetic phase transition temperature of 110 K. Furthermore, the energy bandwidth of this mode is in accordance with that of the acoustic magnon branch observed in YVO_3 (see ref. [9]). The mode at 14.9 meV exhibits a different behaviour. This excitation is dispersionless in energy, linewidth, and intensity. Furthermore, the mode does not completely disappear above the magnetic phase transition. Therefore, this mode cannot be associated with a magnetic excitation. A comparison with the Raman light scattering data obtained on NdVO_3 and LaVO_3 indicates that the lowest energy optical phonon modes should appear at an energy above 20 meV [10]. Thus, this mode cannot be associated with a lattice vibration. Therefore, the excitation at 14.9 meV can be attributed to a crystal field excitation arising from the Tb-moments. From its temperature dependence the weakly dispersive mode between 24.3 meV and 25.6 meV can be attributed to spin excitations. This energy is also in close to that of the optical magnon branch observed in YVO_3 which appears between 16 meV and 20 meV. A weak inelastic signal remains above the magnetic phase transition temperature at an energy of 22 meV. This weak contribution can be associated with the lowest energy optical phonon branch of TbVO_3 and originates from the vibration of the Tb-atoms.

The resulting dispersion relation of the excitation spectrum of TbVO_3 is shown on the left side of Fig. 3. For comparison, the spin wave dispersion and crystal field excitation spectrum of TbMnO_3 , measured by Senff *et al.* [11], is shown on the right. The overall magnon bandwidth of the acoustic magnon branch in TbVO_3 is comparable to the spin excitations in TbMnO_3 . As in YVO_3 , a splitting into an acoustic and an optical magnon branch is observed. The presence of a magnon splitting served as the main argument for the existence of an ‘orbital Peierls state’ in YVO_3 [9,12,13].

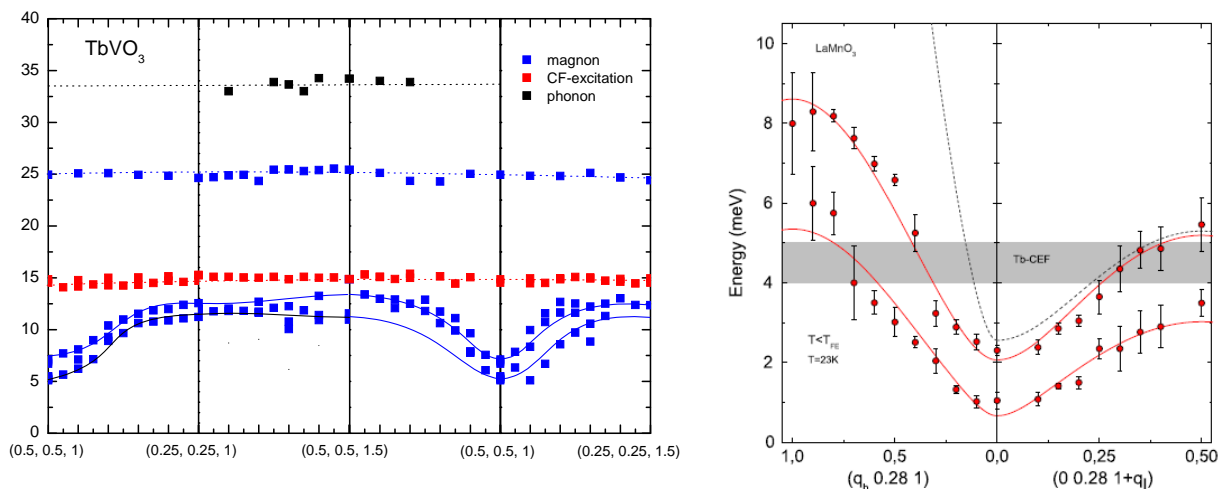


Fig. 3. Spin wave dispersion relation of TbVO_3 taken at 40 K (left). The blue symbols can be associated with spin wave excitations, whereas the black symbols correspond to phonons. The red symbols denote excitations arising from a crystal field excitation of the Tb-ions. For comparison, the spin wave dispersion and crystal field excitation spectrum of TbMnO_3 , measured by D. Senff *et al.* [11], is shown on the right.

4. Conclusions

In conclusion, we have determined the dispersion relation of the excitation spectrum of TbVO_3 . An acoustic and an optical magnon branch are identified at comparable energies as in the spin wave excitation spectrum of YVO_3 . Furthermore, a crystal field excitation arising from the Tb-ions is identified at an energy of 14.9 meV. This is substantially larger than the crystal field excitation at 4.5 meV in isostructural TbMnO_3 . These data can serve as an important input for future calculations of the crystal field excitation spectrum in both TbMnO_3 and TbVO_3 and can thus provide significant information about the electronic and magnetic structures of both materials.

References

- [1] Cheong S-W and Mostovoy M 2007 *Nature Materials* **6** 13
- [2] Eerenstein W, Mathur N D and Scott J F 2006 *Nature* **442** 759
- [3] Kenzelmann M, Harris A B, Jonas S, Broholm C, Schefer J, Kim S B, Zhang C L, Cheong S-W, Vajk O P and Lunn J W 2005 *Phys. Rev. Lett.* **95** 087206
- [4] Aliouane N, Schmalzl K, Senff D, Maljuk A, Prokes K, Braden M and Argyriou 2009 *Phys. Rev. Lett.* **102** 207205
- [5] Miyasaka S Okimoto Y, Iwama M and Tokura Y 2003 *Phys. Rev. B* **68** 100406
- [6] Fujioka J, Miyasaka S and Tokura Y 2005 *Phys. Rev. B* **72** 024460
- [7] Fujioka J, Yasue T, Miyasaka S, Yamasaki Y, Arima T, Sagayama H, Inami T, Ishii K and Tokura Y 2010 *Phys. Rev. B* **82** 144425
- [8] Reehuis M, Ulrich C, Pattison P, Ouladdiaf B, Rheinstädter M C, Ohl M, Regnault P, Miyasaka M, Tokura Y and Keimer B 2006 *Phys. Rev. B* **73** 094440
- [9] Ulrich C, Khaliullin G, Sirker J, Reehuis M, Ohl M, Miyasaka S, Tokura Y and Keimer B 2003 *Phys. Rev. Lett.* **91** 257202
- [10] Miyasaka S, Onoda S, Okimoto Y, Fujioka J, Iwama M, Nagaosa N and Tokura Y 2005 *Phys. Rev. Lett.* **94** 076405
- [11] Senff D, Aliouane N, Argyriou D N, Hiess A, Regnault L P, Link P, Hradil K, Sidis Y and Braden M 2008 *J. Phys. Condens. Matter.* **20** 434212
- [12] Khaliullin G, Horsch P, and Oles A M 2001 *Phys. Rev. Lett.* **86** 3879
- [13] Horsch P, Khaliullin G and Oles A M 2003 *Phys. Rev. Lett.* **91** 257203